Gas-Phase Chiral Separations by Ion Mobility Spectrometry

Prabha Dwivedi,[†] Ching Wu,*,[‡] Laura M. Matz,[†] Brian H. Clowers,[†] William F. Seims,[†] and Herbert H. Hill, Jr.*,[†]

Department of Chemistry and Center for Multiphase Environmental Research, Washington State University, Pullman, Washington 99164, and Excellims Corporation, Maynard, Massachusetts 01754

This article introduces the concept of chiral ion mobility spectrometry (CIMS) and presents examples demonstrating the gas-phase separation of enantiomers of a wide range of racemates including pharmaceuticals, amino acids, and carbohydrates. CIMS is similar to traditional ion mobility spectrometry, where gas-phase ions, when subjected to a potential gradient, are separated at atmospheric pressure due to differences in their shapes and sizes. In addition to size and shape, CIMS separates ions based on their stereospecific interaction with a chiral gas. In order to achieve chiral discrimination by CIMS, an asymmetric environment was provided by doping the drift gas with a volatile chiral reagent. In this study (S)-(+)-2-butanol was used as a chiral modifier to demonstrate enantiomeric separations of atenolol, serine, methionine, threonine, methyl α-glucopyranoside, glucose, penicillamine, valinol, phenylalanine, and tryptophan from their respective racemic mixtures.

Since Louis Pasteur's discovery of the "handedness" of molecules, the development of analytical methods for measuring molecular chirality has been a major focus of separation chemistry. Chirality measurement is important for a wide range of applications including those of proteomics (and related "omics"), pharmacology, health sciences, environmental sciences, space exploration, and geology. Molecular chirality is a fundamental component of drug discovery, one necessary to understand and describe biological targets as well as to design effective pharmaceutical agents. Optically pure isomers are often required to produce a desired therapeutic effect, reduce an undesired side effect and eliminate toxicity.[1,2] In addition to drug discovery, identifying the roll that L- and D-amino acids play in protein structure[3-6] has challenged modern analytical methodology. Chiral modification

of protein structure has been implicated in the formation of cataracts,[7] the aging process,[8,9] neurotransmission, endocrine regulation,[10] cancer,[11] Alzheimer's disease,[12,13] and multiple sclerosis.[14] Enantiomeric ratios have also been used to evaluate the quality of food material,[15,16] to determine the age of fossils and geological strata,[17,18] and to search for extraterrestrial life.[19,20] In forensic medicine, the age of an individual at the time of death can be determined by the ratio of amino acid enantiomers.[21,22] Chirality can also impart aroma differences in certain molecules.[23]

Clearly, chirality is an important component of the chemistry of our world. To probe these chemistries, we need rapid, versatile, sensitive and efficient chiral separation and detection methods. The similarity of enantiomers in their chemical and physical properties, however, makes their separation and detection difficult. Since, 1980 chiral separations have been primarily achieved by chromatography[24] and capillary electrophoresis,[25] while nuclear magnetic resonance spectroscopy[26] has been useful for structure confirmation.

Separation of enantiomers using liquid chromatographic techniques is based on the "three-point rule", also known as the Pirkle rule, which states, "Chiral recognition requires a minimum of three

* Corresponding authors. E-mail: hhhill@wsu.edu. Phone: 509-335-5648. Fax: 509-335-8867. E-mail: ching.wu@excellims.com. Phone: 978-461-6050. Fax: 978-461-6051.

 † Washington State University.

  ‡ Excellims Corp.

(1) Hutt, A. J. In *Smith and Williams' Introduction to the Principles of Drug Design and Action,* 4th ed.; Smith, H. J., Ed.; CRC/Taylor & Francis: Boca Raton, FL, 2006; pp 117−183.

(2) Federsel, H. J. *Chirality* **2003**, *15* (Suppl), S128−142.

(3) Kreil, G. *Annu. Rev. Biochem.* **1997**, *66*, 337−345.

(4) Shapira, R.; Wilkinson, K. D.; Shapira, G. *Prog. Clin. Biol. Res.* **1989**, *292*, 487−496.

(5) Buczek, O.; Yoshikami, D.; Bulaj, G.; Jimenez, E. C.; Olivera, B. M. *J. Biol. Chem.* **2005**, *280*, 4247−4253.

(6) Fujii, N. *Origins Life Evol. Biospheres* **2002**, *32*, 103−127.

(7) Masters, P. M.; Bada, J. L.; Zigler, J. S., Jr. *Nature* **1977**, *268*, 71−73.

(8) Helfman, P. M.; Bada, J. L. *Nature* **1976**, *262*, 279−281.

(9) Dunlop, D. S.; Neidle, A.; McHale, D.; Dunlop, D. M.; Lajtha, A. *Biochem. Biophys. Res. Commun.* **1986**, *141*, 27−32.

(10) Fuchs, S. A.; Berger, R.; Klomp, L. W. J.; de Koning, T. J. *Mol. Genet. Metab.* **2005**, *85*, 168−180.

(11) Kogl, F.; Erxleben, H. *Nature (London)* **1939**, *144*, 111.

(12) Kubo, T.; Kumagae, Y.; Miller, C.; Kaneko, I. *J. Neuropathol. Exp. Neurol.* **2003**, *62*, 248[NLM - MEDLINE].

(13) Takahiko, S.; Fukuda, H.; Murayama, S.; Izumiyama, N.; Shirasawa, T. *J. Neurosci. Res.* **2002**, *70*, 451−461.

(14) Fisher, G. H.; Petrucelli, L.; Gardner, C.; Emory, C.; Frey, W. H. n.; Amaducci, L.; Sorbi, S.; Sorrentino, G.; Borghi, M.; D'Aniello, A. *Mol. Chem. Neuropathol.* **1994**, *23*, 2−3.

(15) Marchelli, R.; Dossena, A.; Palla, G. *Trends Food Sci. Technol.* **1996**, *7*, 113−119.

(16) Masters, P. M.; Friedman, M. *J. Agric. Food Chem.* **1979**, *27*, 507−511.

(17) Masters, P. M.; Zimmerman, M. R. *Science* **1978**, *201*, 811−812.

(18) Bada, J. L.; Protsch, R. *Proc. Natl. Acad. Sci. U. S. A.* **1973**, *70*, 1331−1334.

(19) Bada, J. L. *Science* **1997**, *275*, 942−943.

(20) Kvenvolden, K. *Nature* **1970**, *228*, 923−926.

(21) Helfman, P. M.; Bada, J. L. *Proc. Natl. Acad. Sci. U.S.A.* **1975**, *72*, 2891−2894.

(22) Masters, P. M. *Forensic Sci. Int.* **1986**, *32*, 179−184.

(23) Russell, G. F.; Hills, J. I. *Science* **1971**, *172*, 1043−1044.

(24) Zhang, Y.; Wu, D.-R.; Wang-Iverson, D. B.; Tymiak, A. A. *Drug Discovery Today* **2005**, *10*, 571−577.

(25) Gubitz, G.; Schmid, M. G. *J. Chromatogr., A* **1997**, *792*, 179−225.

(26) Freire, F.; Seco, J. M.; Quiñóa, E.; Riguera, R. *Chem.−Eur. J.* **2005**, *11*, 5509−5522.

simultaneous interactions between the chiral stationary phase and at least one of the enantiomers, with at least one of the interactions being stereochemically dependent. That is, at least one of the interactions will be absent or significantly altered by replacing one enantiomer with the other without conformational change in any component."[27,28]

In chromatography, using a chiral stationary phase, the enantiomer that forms the more stable association with the chiral selector will be the more strongly retained species of the mixture. On the other hand, a chiral mobile phase reduces the retention of the solute enantiomer that forms a stronger association with the chiral selector. The major problem with chromatographic separation techniques is that the optimal separation condition is compound specific,[29] which results in time-consuming and costly method development steps for each compound. For example, over 1000 chiral stationary phases are commercially available for HPLC, yet there is no clear method to determine which phase will provide the best separation.

In an effort to eliminate the slow and tedious steps of enantiomer separation by chromatography, mass spectrometric methods have been developed for chiral discrimination. The validity of the "three-point interaction" model in gas phase has been examined by many research groups.[30−32] The "guest" exchange reaction between a chiral selector−chiral analyte complex and a volatile chiral compound or a chiral gas using Fourier transform ion cyclotron resonance mass spectrometry, Fourier transform mass spectrometry, quadrupole ion trap mass spectrometry has been investigated. The chiral/achiral gas was infused in the ion cyclotron resonance/ion trap cell at low pressures and the binding energy of the trimeric complex of chiral selector−chiral complex−chiral/achiral gas was measured. Ahn et al. studied the guest exchange reaction between a cyclodextrin−amino acid complex and a gaseous alkylamine and concluded that the three-point interaction model is indeed valid in the gas phase. It was also suggested that enantioselectivity is optimal when two points of attraction and one point of repulsion are present in the gas-phase complex.[33] At present, several mass spectrometric methods have been developed for enantiomer discrimination including host−guest adduct formation,[34−36] ion−molecule reactions,[37,38] collision-induced dissociation of diastereomeric adducts,[39,40] gas-phase kinetics,[41,42] and solution-phase kinetic reso-
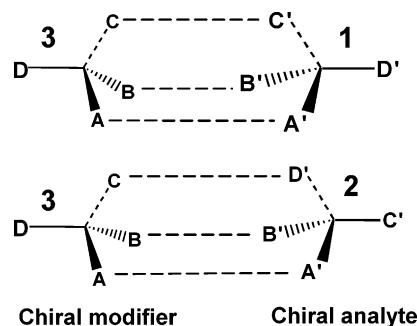
Figure 1. Schematic illustrating the three-point "Pirkle Rule" required for chiral recognition. CIMS separation utilizes stereochemically different noncovalent interactions between the enantiomers (1 and 2) and the chiral modifier (3).

lution.[43,44] However, these approaches often require ion−molecule reactions to occur between the chiral selector and the ion of interest along with complex data analysis of fragmentation patterns. Unfortunately, mass spectrometric approaches for chiral discrimination are not yet routine, and for most applications, research and development is still in its infancy.

Since the 1980s, our group has been investigating the effects of alternative drift gases on the separation of gas-phase ions by ion mobility spectrometry.[45] To explore the possibility of obtaining structure information from IMS measurements, Jarrold and Bowers studied the effect of long-range potentials on ion mobility measurements in a pure "buffer gas".[46,47] More recently, we have demonstrated that relative mobilities change as a function of drift gas and that unique separations can be achieved by varying the drift gas.[48,49] While these investigations demonstrated that using different drift gases can change ion mobilities of analyte ions, there have been no studies to investigate long-range potential effects on the mobilities of chiral compounds.

The concept of chiral ion mobility spectrometry (CIMS) is as follows. As depicted schematically in Figure 1, CIMS utilizes stereospecific long-range interaction forces between chiral analyte ions (1 and 2) and a neutral chiral molecule (3) (chiral modifier) to achieve resolution of enantiomeric ions in the gas phase. By exposing ions to a "chiral modifier", selective ion−molecule interactions through which the identity of the analytes is not lost and a true chiral separation of enantiomers may be achieved. This approach differs significantly from MS chiral differentiation techniques that rely on the formation of clusters and subsequent fragmentation of these clusters.

In preliminary experiments, using atmospheric pressure ion mobility time-of-flight mass spectrometry, we demonstrated weak

(27) Pirkle, W. H.; Pochapsky, T. C. *Chem. Rev.* **1989**, *89*, 347−362.
(28) Pirkle, W. H.; Finn, J. M.; Hamper, B. C.; Schreiner, J.; Pribish, J. R. *ACS Symp. Ser.* **1982**, *185*, 245−260.
(29) Fulde, K.; Frahm, A. W. *J. Chromatogr., A* **1999**, *858*, 33−43.
(30) Grigorean, G.; Gronert, S.; Lebrilla, C. B. *Int. J. Mass Spectrom,* **2002**, *219*, 79−87.
(31) Jürg, M. D.; Friess, S. D.; Rajagopalan, S.; Wendt, S.; Zenobi, R. *Int. J. Mass Spectrom.* **2002**, *216*, 1−27.
(32) Filippi, A.; Giardini, A.; Piccirillo, S.; Speranza, M. *Int. J. Mass Spectrom.* **2000**, *198*, 137−163.
(33) Ahn, S.; Ramirez, J.; Grigorean, G.; Lebrilla, C. B. *J. Am. Soc. Mass Spectrom.* **2001**, *12*, 10.
(34) Chu, I. H.; Dearden, D. V.; Bradshaw, J. S.; Huszthy, P.; Izatt, R. M. *J. Am. Chem. Soc.* **1993**, *115*, 4318−4320.
(35) Pocsfalvi, G.; Liptak, M.; Huszthy, P.; Bradshaw, J. S.; Izatt, R. M.; Vekey, K. *Anal. Chem.* **1996**, *68*, 792−795.
(36) Mathias, S. *Angew. Chem., Int. Ed.* **2003**, *42*, 1896−1899.
(37) Grigorean, G.; Cong, X.; Lebrilla, C. B. *Int. J. Mass Spectrom.* **2004**, *234*, 71−77.
(38) Hua, S.; Chen, Y.; Jiang, L.; Xue, S. *Org. Mass Spectrom.* **1986**, *21*, 7−10.
(39) Filippi, A.; Gasparrini, F.; Pierini, M.; Speranza, M.; Villani, C. *J. Am. Chem. Soc.* **2005**, *127*, 11912−11913.
(40) Mancel, V.; Sellier, N.; Lesage, D.; Fournier, F.; Tabet, J.-C. *Int. J. Mass Spectrom.* **2004**, *237*, 185−195.
(41) Wu, L.; Andy Tao, W.; Cooks, R. G. *J. Mass Spectrom.* **2003**, *38*, 386−393.
(42) Bagheri, H.; Chen, H.; Cooks, R. G. *Chem. Commun.* **2004**, 2740−2741.
(43) Hashimoto, K.; Sumida, Y.; Terada, S.; Okamura, K. *J. Mass Spectrom. Soc. Jpn.* **1993**, *41*, 87−94.
(44) Gong, S.; Camara, E.; He, F.; Green, M. K.; Lebrilla, C. B. *Int. J. Mass Spectrom.* **1999**, *185−187*, 401−412.
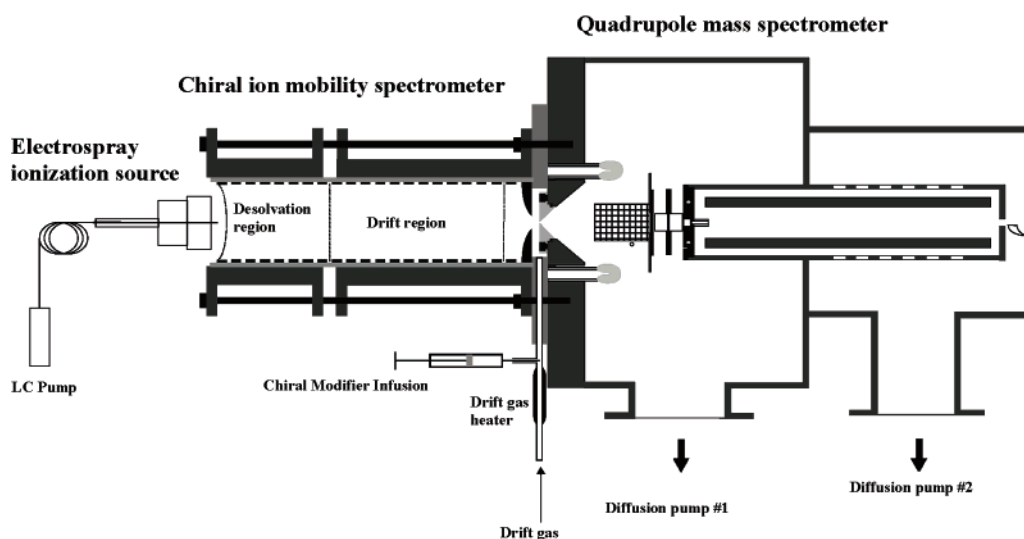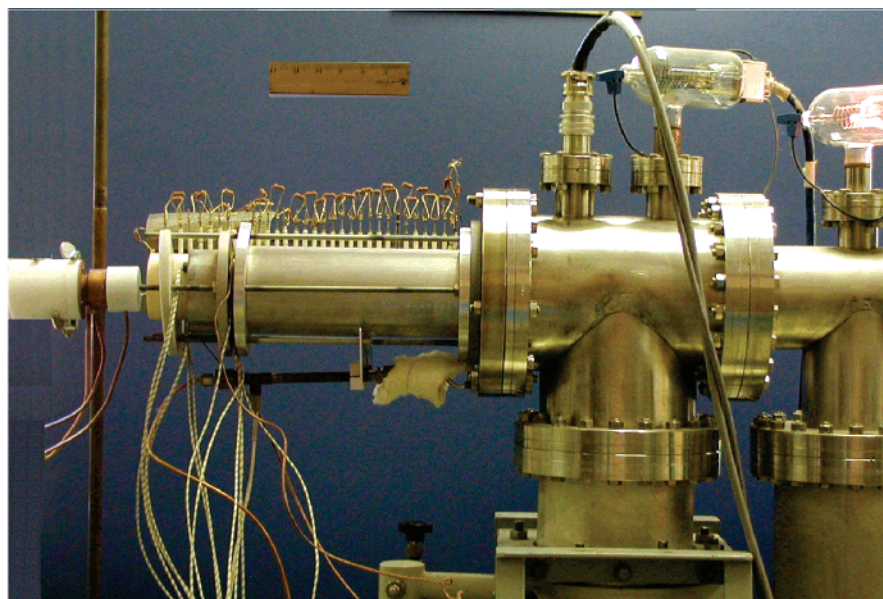(45) Rokushika, S.; Hatano, H.; Hill, H. H. *J. Anal. Chem.* **1986**, *58*, 361−365.
(46) Mesleh, M. F.; Hunter, J. M.; Shvartsburg, A. A.; Schatz, G. C.; Jarrold, M. F. *J. Phys. Chem.* **1996**, *100*, 16082−16086.
(47) Wyttenbach, T.; Helden, G. v.; Batka, J. J. J.; Carlat, D.; Bowers, M. T. *J. Am. Soc. Mass Spectrom.* **1997**, *8*, 275−282.
(48) Matz, L. M.; Hill, H. H. J.; Beegle, L. W.; Kanik, I. *J. Am. Soc. Mass Spectrom.* **2002**, *13*, 300−307.
(49) Asbury, G. R.; Hill, H. H. *Anal. Chem.* **2000**, *72*, 580−584.

Figure 2. Photograph and schematic diagram of the electrospray ionization-atmospheric pressure ion mobility mass spectrometer. The IMS cell was divided into a desolvation region (7.5 cm) and a drift region (25 cm) by a Bradbury−Nielsen ion gate, which was used to pulse ion packets into the drift region with a pulse width of 0.1 ms. The Q-MS was operated in single ion monitoring mode to monitor the arrival time distributions of mass-selected ions.

gas-phase interactions, which might lead to enantiomeric separations.[50] Environmental factors, specifically, temperature and drift gas composition, were varied. The reduced mobility values (K_o) of two enantiomers, L- and D-amphetamine, obtained at varying chiral modifier concentrations ((R)- and (S)-2-butanol), indicated the occurrence of a preferential shift in mobility between the two enantiomers. In this paper, we demonstrate the first gas-phase separation and resolution of enantiomers by ion mobility spectrometry.

EXPERIMENTAL SECTION

Chemicals. Enantiomers (R)/(S)-atenolol, D/L-serine, D/L-methionine, D/L-threonine, D/L-penicillamine, D/L-valinol, D/L-phenylalanine, and D/L-tryptophan were purchased from Sigma-

Aldrich Chemical Co. Inc. (Milwaukee, WI) and were classified as ACS reagent grade with ≥98% purity. D/L-Methyl α-glucopyranoside was kindly donated by Dr. Brad A. Bendiak of Cell and Development Biology, University of Colorado Health Sciences Center. Chiral modifiers ((S)-(+)-2-butanol and (R)-(−)-2-butanol) with enantiomeric purity of 99% were also purchased from Sigma-Aldrich Chemical Co.

Ion Mobility Mass Spectrometer (IMMS). Experiments were carried out in an atmospheric pressure ion mobility spectrometer interfaced with a 40-μm pinhole to a quadrupole mass spectrometer. A photograph and a schematic drawing of the instrument are shown in Figure 2. This IMMS was constructed at Washington State University (Pullman, WA) and operated in the positive ion mode. Earlier publications from our research group document the detailed description and schematics of this IMMS.[51,52] A brief overview of the instrument is provided below.

(50) Clowers, B. H.; Wu, C.; Matz, L. M.; Steiner, W. E.; Siems, W. F.; Hill, H. H. 50th Annual American Society of Mass Spectrometry (ASMS) Conference; Orlando, FL, 2002.
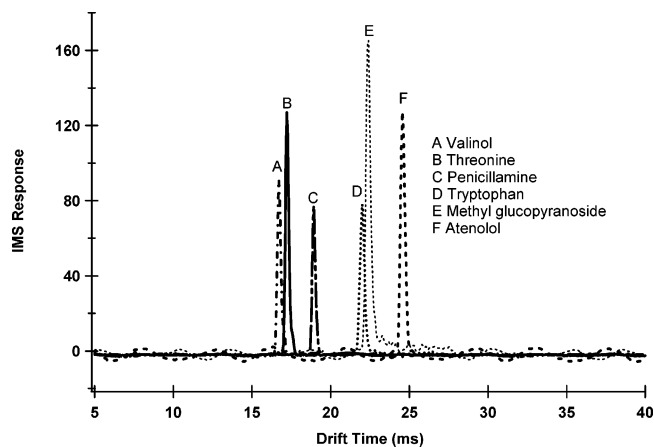
The IMS was divided into two regions, the desolation region (7.5 cm in length) and the drift region (25.05 cm in length), which were separated by a Bradbury−Nielsen-style ion gate. Ions were pulsed into the drift region with a width of 0.1 ms. Both regions consisted of alternating alumina spacers and stainless steel rings with high-temperature resistors connecting the stainless steel rings (500-kΩ resistors for the desolation region, 1-MΩ resistors for the drift region). The temperature of the drift region, the desolation region, and the drift gas was maintained at 200 °C, the ion gate was held at a voltage of 10.8 kV (electric field (E) = 432 V/cm, number density (N) = 1.43×10^{19}, E/N = 3.02 Townsend), and the instrument was operated at atmospheric pressure (694−705 Torr in Pullman, WA). A preheated counter-flowing nitrogen drift gas at a flow rate of ∼1 L/min was introduced at the end of the drift region.

The IMS was interfaced to a model 150-QC ABB Extrel (Pittsburgh, PA) quadrupole MS (m/z range of 0−4000 amu) via a 40-μm pinhole interface. The output signal from the multiplier was amplified by a Keithley model 427 amplifier (Keithley Instruments, Cleveland, OH). The amplified signal was then sent to either the MS data acquisition system or IMS acquisition system. Merlin software (ABB Extrel, Pittsburgh, PA) was utilized for all mass spectral analyses and mass spectrometer control. For the IMS gating and data acquisition, the electronic controls were built at Washington State University. The data acquisition and IMS gate control software employed was Labview-based (National Instruments, Austin, TX) and was developed at Washington State University. Ion mobility spectra were obtained in two ways: total ion monitoring or mass-selective ion monitoring (SIM). In the first case, the IMS was continually gated and the MS was operated in the rf-only mode with the dc voltage turned off. In the SIM mode, the quadrupole was operated with the dc voltage on to allow ions with a specific m/z to pass through the MS.

Introduction of Chiral Samples and Drift Gas Modifier. For the reported results, electrospray ionization (ESI) was used as the ionization source with an ESI solution of 47.5% methanol + 47.5% water + 5% acetic acid. Standard solutions of the individual enantiomers and the racemic mixtures were prepared in an ESI solution. The mixing ratio of the sample to the ESI solution was 100 parts per million (ppm). The ESI solvent with or without the analytes was pumped by a KD Scientific (New Hope, PA) 210 syringe pump at a flow rate of 3 μL/min into a 20-cm-long, 50-μm-inner diameter silica capillary. This capillary was then connected to a 15-cm-long, 50-μm-inner diameter silica capillary through a stainless steel junction. The other end of the 15-cm capillary was centered ∼5 mm from the target screen of the IMS. The target screen was made of a 2-mm stainless steel mesh with a hole in the center of the 0.5-cm radius. A positive high voltage of 15.00 kV was applied at the steel junction to generate positively charged ions in the electrospray.

Heated nitrogen was used as drift gas and (S)-(+)-2-butanol (FW 74.12, bp 99−100 °C) or (R)-(−)-2-butanol (FW 74.12, bp 97−100 °C) was used as the chiral drift gas modifier. The chiral modifiers were infused by a KD Scientific 210 syringe pump through a 30-cm-long, 50-μm-inner diameter silica capillary into

(51) Wu, C.; Siems, W. F.; Asbury, G. R.; Hill, H. H. *Anal. Chem.* **1998**, *70*, 4929−4938.
(52) Asbury, G. R.; Hill, H. H. *J. Microcolumn Sep.* **2000**, *12*, 172−178.

Figure 3. Superimposed ion mobility spectra of racemic mixtures in nitrogen drift gas. The figure shows that racemic mixtures of enantiomers drifted with same mobility in pure nitrogen as drift gas. Mixtures represented in the spectra above are those of valinol, threonine, penicillamine, tryptophan, methyl α-D-glucopyranoside, and atenolol. Each enantiomer was present in the electrospray solution at a mixing ration of 100 ppm. Samples were introduced into IMS from the electrospray at a rate of 3 μL/min. Experiments were repeated three separate times, and the average standard deviation of the drift time measurement was 0.04 ms.

the nitrogen drift gas line using a T-junction, 5 cm before the drift gas inlet into the IMS as schematically shown in Figure 2.

RESULTS AND DISCUSSION

Ion mobility spectra of individual enantiomers and their racemic mixtures were acquired by collecting the IMS spectra while operating the mass spectrometer in the single ion monitoring mode. In this mode of operation, ions of only one m/z (mass-to-charge ratio) value were allowed to traverse the mass analyzer. Enantiomer separation by IMS was achieved when two IMS peaks were observed for one m/z value and the drift times of the peaks corresponded to the drift times of the individual enantiomers. Figure 3 shows the superimposed IMS spectra of racemic mixtures of valinol, threonine, penicillamine, tryptophan, methyl α-D-glucopyranoside, and atenolol with nitrogen as the drift gas. With only nitrogen as the drift gas (no chiral modifier added), separation of the enantiomers was not observed since the drift times of the individual enantiomers and the racemic mixture for each analyte were identical within a maximum standard deviation of 0.05 ms.

To determine the amount of chiral modifier needed in the drift gas to achieve chiral separation, arrival times (drift times) of the enantiomers of methionine in a racemic mixture were monitored as a function of the chiral modifier mixing ratio in the inert drift gas. Chiral modifiers ((S)-(+)-2-butanol and (R)-(−)-2-butanol) were doped into the drift gas stream one at a time. In pure nitrogen, the drift times of the methionine enatiomers were identical at 21.52 ± 0.04 ms. (S)-(+)-2-Butanol or (R)-(−)-2-butanol was introduced into the nitrogen drift gas line at increments of 1 μL/h. A 1 μL/h injection of liquid butanol into the nitrogen drift gas was equivalent to a 0.22 ppm volume-to-volume mixing ratio in the nitrogen drift gas, assuming complete volatilization and mixing with the nitrogen drift gas. The variation of drift time of the methionine enantiomers with the modifier introduction rate of (S)-(+)-2-butanol or (R)-(−)-2-butanol is shown in Figure 4.
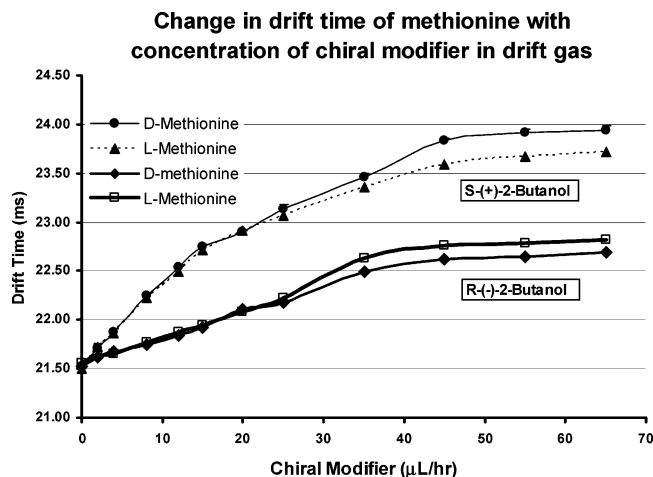
Figure 4. Effect of chirality and flow rate of the modifier on the arrival times of the methionine enantiomers. The figure shows retardation in mobility of methionine enantiomers with increasing concentration of either (*S*)-(+)-2-butanol or (*R*)-(−)-2-butanol as the chiral modifiers in nitrogen drift gas. Better separation of enantiomers was observed with (*S*)-(+)-2-butanol as the chiral modifier (separation factor of 1.01) as compared to (*R*)-(−)-2-butanol (separation factor of 1.006). The order of elution of methionine enantiomers was reversed for the two modifiers. Optimal flow rate of the chiral modifier was ~45 μL/h, which corresponded to ~10 ppm chiral modifier in the nitrogen drift gas. Each experiment was repeated three times, and the standard deviation of the arrival times varied by ~2%. These error bars are too small to be seen in the figure.

Experiments were repeated three separate times, and the average standard deviation of the drift time measurement was 0.04 ms.

At the chiral modifier introduction rate of 5 μL/h (~1 ppm), the drift time of the methionine enatiomers shifted to 22.12 ms with (*S*)-(+)-butanol and to 21.66 ms with (*R*)-(−)-2-butanol, but no separation in the peaks was observed. A single IMS peak for the racemate was observed up to a chiral modifier introduction rate of 25 μL/h (~5 ppm). With subsequent increases in the chiral modifier concentration, the enantiomers began to separate. The maximum separation factor between the two enantiomers was 1.01 at a flow rate of 45 μL/h (~10 ppm) (*S*)-(+)-2-butanol (separation factor, α-value = t_{d2}/t_{d1}; t_{d2} is the drift time of the longer drifting ion and t_{d1} is the drift time of the shorter drifting ion). At this flow rate, the drift times were 23.83 ± 0.03 ms for D-methionine and 23.59 ± 0.04 ms for L-methionine. With increasing mixing ratio of (*S*)-(+)-2-butanol in the inert drift gas, the ion velocity of methionine decreased, suggesting increased ion−chiral modifier interactions. However, no significant change in separation factor was observed beyond the introduction rate of 45μL/h (*S*)-(+)-2-butanol. More detailed parametric experiments, coupled with modeling the interaction potentials and collision frequencies, will be required to understand why the drift time did not continue to shift linearly with increasing dopant concentration.

A smaller shift in drift time was observed with (*R*)-(−)-2-butanol as the chiral modifier with maximum separation factor of 1.006 between the enantiomers with drift times of 22.49 ± 0.04 ms for D-methionine and 22.63 ± 0.03 ms for L-methionine. As expected, with (*R*)-(−)-2-butanol, the elution order of L-methionine and D-methionine was reversed with L-methionine drifting longer than D-methionine. The identities of the isomers were made by measuring the drift time of each enantiomer under identical
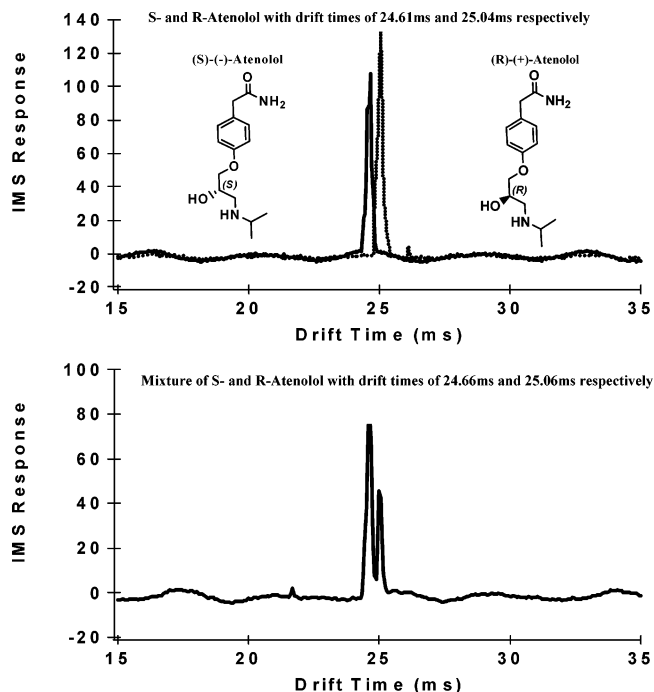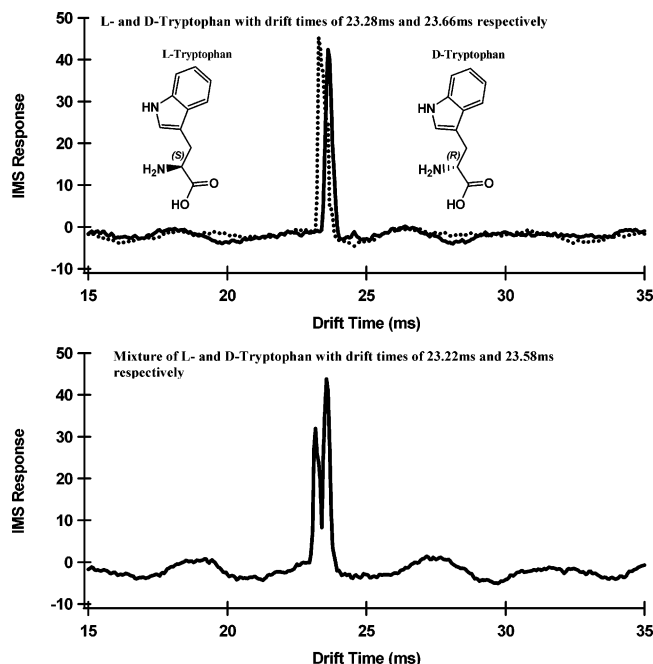

Figure 5. Gas-phase separation of atenolol enantiomers. The upper graph shows the superimposed spectrum of (*S*)- and (*R*)-atenolol obtained after introduction 10 ppm (*S*)-(+)-2-butanol as the chiral modifier in the inert nitrogen drift gas. The bottom graph demonstrates the separation of the enantiomers from their racemic mixture. An average standard deviation of 0.05 ms in drift times was measured from three separate ion mobility measurements.

experimental conditions and a modifier introduction rate of 45 μL/h (~10 ppm).

Ion mobility separation was also possible for a variety of racemates. CIMS separation of (*R*)- and (*S*)-atenolol enantiomers from its racemic mixture is illustrated in Figure 5. Atenolol is from a class of drugs called β-blockers mainly prescribed alone or in combination with other medications to treat high blood pressure, to lower the heart rate, to prevent angina, and to reduce the risk of recurrent heart attacks. Drift times of (*S*)- and (*R*)-atenolol were measured to be 24.61 ± 0.04 and 25.04 ± 0.05 ms, respectively, when analyzed individually. Enantiomers (*S*)- and (*R*)-atenolol had drift times of 24.66 ± 0.04 and 25.06 ± 0.05 ms, respectively, when a racemic mixture of atenolol was separated by CIMS.

Separation of enantiomers of tryptophan by CIMS is demonstrated in Figure 6. The upper spectra in Figure 6 show the drift times of L- and D-tryptophan (23.28 ± 0.04 and 23.66 ± 0.04 ms, respectively), when analyzed individually. The bottom spectrum of Figure 6 shows the separation of the enantiomers from a mixture of L- and D-tryptophan with drift times of 23.22 ± 0.05 and 23.58 ± 0.05 ms, respectively.
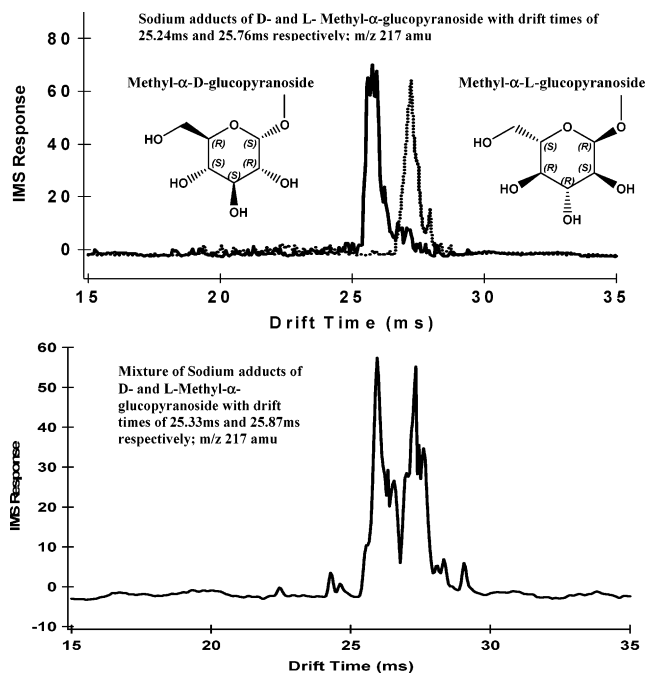
Figure 7 illustrates the CIMS separation of sodium adducts of D- and L-methyl α-glucopyranoside enantiomers. The upper graph shows the superimposed spectra of D- and L-methyl α-glucopyranoside enantiomers analyzed individually and obtained after introduction of (*S*)-(+)-2-butanol as the chiral modifier into the inert drift gas. Sodium adducts of D- and L-methyl α-glucopyranoside were observed at an *m/z* value of 217 amu and drift times of 25.24 ± 0.06 and 25.76 ± 0.05 ms, respectively. With drift times of 25.33 ± 0.08 and 25.87 ± 0.07 ms, respectively, separation of

Figure 6. Ion mobility spectra illustrating the gas-phase separation of tryptophan enantiomers. The upper graph shows the superimposed spectrum of L- and D-tryptophan obtained after introduction of 10 ppm (S)-(+)-2-butanol as the chiral modifier in the inert nitrogen drift gas. The bottom graph demonstrates the separation of the enantiomers from their racemic mixture. Experiments were repeated three separate times, and the average standard deviation of the drift time measurement was 0.05 ms.

Figure 7. Ion mobility spectra illustrating the gas-phase separation of sodium adduct of D- and L-methyl α-glucopyranoside enantiomers. The upper graph shows the superimposed spectrum of D- and L-methyl α-glucopyranoside enantiomers obtained after introduction of 10 ppm (S)-(+)-2-butanol as the chiral modifier in the inert nitrogen drift gas. The bottom graph demonstrates the separation of the enantiomers from their racemic mixture. An average standard deviation of 0.07 ms in drift time was measured from triplicate ion mobility measurements.

D- and L-methyl α-glucopyranoside enantiomers from their racemic mixture is demonstrated in the bottom graph of Figure 7.

Other examples of enantiomer separation, including threonine, valinol, and penicillamine, by chiral IMS are reported in Table 1. CIMS separations of enantiomers of atenolol, serine, methionine, threonine, methyl α-glucopyranoside, glucose, penicillamine, valinol, phenylalanine, and tryptophan from their respective racemic mixtures are summarized in the table. The mass-to-charge ratio of the ion monitored for mobility measurements is listed in column 1. Chirality of each enantiomer is shown in parentheses in columns

3 and 4. The drift time of each enantiomer in pure nitrogen is listed in column 3 and in nitrogen + 10 ppm (S)-(+)-2-butanol in column 4. Reduced mobilities determined for each enantiomer are reported in columns 5 and 6 in the units of centimeter squared per volt·second. Standard deviations in drift time were calculated from three measurements. When nitrogen was used as the drift gas, drift times (and thus reduced mobilities) of the enantiomers were not statistically different and had the same reduced mobility values. However, when the drift gas was doped with the chiral

Table 1. Drift Times and Mobility Constants of Enantiomers in Nitrogen and Nitrogen Plus 10 ppm Chiral Modifier as Drift Gases[a]

mol wt of ion (amu) measured and ion identity	test compounds	drift time (ms) of enantiomers in N_2	drift time (ms) of enantiomers in N_2 + 10 ppm (S)-(+)-2-butanol	K_o value (cm^2/V·s) of enantiomers in N_2		K_o value (cm^2/V·s) of enantiomers in N_2 + 10 ppm (S)-(+)-2-butanol	
267 (M+H)$^+$	(R)- and (S)-atenolol	(S), 24.56 ± 0.03 (R), 24.51 ± 0.03	(S), 24.66 ± 0.04 (R), 25.06 ± 0.05	1.18	1.18	1.18	1.16
205 (M+H)$^+$	D- and L-tryptophan	(D), 22.02 ± 0.03 (L), 21.99 ± 0.04	(D), 23.22 ± 0.05 (L), 23.63 ± 0.05	1.32	1.32	1.25	1.23
150 (M+H)$^+$	D- and L-methionine	(D), 18.61 ± 0.04 (L), 18.66 ± 0.04	(D), 23.64 ± 0.04 (L), 23.83 ± 0.06	1.56	1.56	1.23	1.22
120 (M+H)$^+$	D- and L-threonine	(D), 17.22 ± 0.03 (L), 17.20 ± 0.04	(D), 19.22 ± 0.05 (L), 19.61 ± 0.05	1.69	1.69	1.51	1.48
217 (M+Na)$^+$	D- and L-methyl α-glucopyranoside	(D), 22.42 ± 0.05 (L), 22.40 ± 0.05	(D), 25.33 ± 0.08 (L), 25.87 ± 0.07	1.30	1.30	1.15	1.12
203 (M+Na)$^+$	D- and L- glucose	(D), 22.35 ± 0.04 (L), 22.32 ± 0.03	(D), 23.61 ± 0.05 (L), 23.98 ± 0.04	1.30	1.30	1.23	1.21
150 (M+H)$^+$	D- and L-penicillamine	(D), 18.94 ± 0.03 (L), 18.92 ± 0.05	(D), 20.48 ± 0.03 (L), 20.78 ± 0.04	1.53	1.53	1.42	1.40
104 (M+H)$^+$	D- and L-valinol	(L), 16.72 ± 0.04 (D), 16.75 ± 0.03	(L), 17.84 ± 0.04 (D), 18.26 ± 0.04	1.74	1.74	1.62	1.60
166 (M+H)$^+$	D- and L-phenylalanine	(L), 20.07 ± 0.04 (D), 20.05 ± 0.04	(D), 22.22 ± 0.03 (L), 22.61 ± 0.05	1.45	1.45	1.31	1.28
106 (M+H)$^+$	D- and L-serine	(D), 16.82 ± 0.03 (L), 16.83 ± 0.04	(D), 18.72 ± 0.04 (L), 19.11 ± 0.05	1.73	1.73	1.55	1.52

[a] Column 1 reports the mass of the ions tested; column 2 identifies the test compounds; column 3 shows their drift times in nitrogen; column 4 shows their drift times in nitrogen plus 10 ppm (S)-(+)-2-butanol; columns 5 and 6 give their reduced mobility values, respectively. These data demonstrate that drift times of all ions are retarded in the chiral drift gas compared to those in nitrogen but that one enantiomer is always retarded more than the other. Standard deviations in drift times were measured from three separate ion mobility measurements.

modifier, drift times and reduced mobility values of each enantiomer were statistically different. All enantiomeric pairs investigated in these experiments separated in the gas phase. Although the experiments and results reported here are preliminary in nature and the mechanism of separation has not been modeled, the phenomenon appears to be universal and applicable for the rapid separation of a wide variety of enantiomeric pairs.

All of the enantiomers used in this study were relatively small molecules with single chiral sites. The effect that chiral modifiers in the drift gas will have on the separation of diastereomers and larger molecular weight compounds is not clear. Peptides and proteins for example have many chiral centers, but due to their molecular structure, steric hindrance can limit the ability of a chiral modifier to satisfy the "Pirkle rule". It has already been demonstrated that a peptide incorporating an L-amino acid can be separated from one with all D-amino acids, but this was due to a kink in the structure at the L-amino acid site causing a size difference in the peptide and was not due to a true chiral separation.[53]

Maximum displacement in the drift time was observed for methionine (~5.2 ms) with (S)-(+)-2-butanol as the chiral modifier as compared to its drift time in nitrogen only. This suggested that methionine had the highest interaction with the chiral modifier as compared to the other enantiomer pairs. Minimum displacement was observed for atenolol, which was ~0.6 ms. Even though methionine experienced maximum interaction in the chiral modified drift gas, the difference in the drift times of the enantiomers was the least among the enantiomers investigated. Maximum difference in the drift times between the enantiomeric pair was observed between D- and L-methyl α-glucopyranoside and D- and L-serine. The IMS peak width of the methyl α-glucopyranoside enantiomers was highest among the samples analyzed. On average, a 2% deviation in drift times between the enantiomers was observed with the chiral modifier added into the drift gas. Drift times of all enantiomeric pairs were statistically same in a drift gas without a chiral modifier.

Because IMS is primarily a method that separates ions based on their collision cross sections, this 2% deviation in drift time as a function of chirality is of considerable theoretical interest. One would think that the size of an ion (its collision cross section) would not be modified merely as a function of its chirality. Thus,

this study is perhaps the first time that ions of the same size have been separated by IMS, demonstrating that when long-range interaction potentials can be selectively applied, mobilities are not directly related to the size of the ion. Although the quantitative determination of collision cross sections is one of the strengths of IMS, long-range interaction potentials complicate those measurements. Nevertheless, for analytical purposes, it appears that prudent application of long-range interaction potentials can effect unique gas-phase ion separations not previously possible.

CONCLUSIONS

Gas-phase separation and resolution of enantiomers is possible when the drift gas of an ion mobility spectrometer is modified with a chiral vapor. Selective interactions occur between the enantiomers and the chiral modifier such that the individual enantiomers have different gas-phase ion mobilities through the spectrometer and can be separated in time. In all cases, the addition of the chiral modifier to the drift gas reduced the mobility of both enantiomers, but the mobility of one enantiomer was always reduced more than that of the other, enabling enantiomer separation.

The data from these experiments are quite encouraging for the development of a novel and rapid analytical method for the measurement of chirality. With a relative limited set of experiments, unoptimized experimental parameters, and a single chiral drift gas modifier, separations of multiple pairs of enantiomers from four different classes of compounds were achieved. Further investigations to elucidate the separation mechanism and optimize operating conditions should result in an analytical technique by which rapid determination of the chirality of molecules may be achieved for a wide range of industrial, environmental, and biomedical applications.

(53) Wu, C.; Siems, W. F.; Klasmeier, J.; Hill, H. H. *Anal. Chem.* **2000**, *72*, 391–395.